Original Article
International Journal of Fuzzy Logic and Intelligent Systems
Vol. 14, No. 4, December 2014, pp. 305-312
http://dx.doi.org/10.5391/IJFIS.2014.14.4.305

ISSN(Print) 1598-2645
ISSN(Online) 2093-744X

Real-Time Peak Shaving Algorithm Using Fuzzy Wind Power Generation Curves for Large-Scale Battery Energy Storage Systems

Subin Son and Hwachang Song
Department of Electrical and Information Engineering, Seoul Nationall University of Science & Technology, Seoul, Korea

Abstract

This paper discusses real-time peak shaving algorithms for a large-scale battery energy storage system (BESS). Although several transmission and distribution functions could be implemented for diverse purposes in BESS applications, this paper focuses on a real-time peak shaving algorithm for an energy time shift, considering wind power generation. In a high wind penetration environment, the effective load levels obtained by subtracting the wind generation from the load time series at each long-term cycle time unit are needed for efficient peak shaving. However, errors can exist in the forecast load and wind generation levels, and the real-time peak shaving operation might require a method for wind generation that includes comparatively large forecasting errors. To effectively deal with the errors of wind generation forecasting, this paper proposes a real-time peak shaving algorithm for threshold value-based peak shaving that considers fuzzy wind power generation.

Keywords: Battery energy storage systems, Energy time shift, Fuzzy wind power generation curves, Peak shaving, Real-time operation

Received: Nov. 10, 2014
Revised : Nov. 27, 2014
Accepted: Dec. 5, 2014

Correspondence to: Hwachang Song
(hcsong@seoultech.ac.kr)

1. Introduction

Recently, we have been being experiencing a severe climate change because of increased CO_2 emission rates resulting from the increased energy demand for industrial development. Several organizations around the world are looking for various ways to solve this problem. One solution might be the application of energy storage systems, which can play an important role in actively coping with the problem resulting from the variability of renewable energy resources, by storing energy that can later be consuming as needed. This paper focuses on the application of a battery energy storage system (BESS).

A BESS has several functions [1-4] that can be implemented to support a transmission and distribution grid. Among these, suppressing the peak load demand and equalizing the load levels with a large-scale BESS is a long-term cycle application. This function is referred to as an energy time shift. In the daily load curve for a system, there is a difference between the peak and minimum load levels. Another long-term cycle function of system marginal price (SMP)-based shaving can be implemented by a wholesale purchasing agency to maximize the benefit from charging and discharging schedules.

Power management systems (PMSs) for a large-scale BESS were proposed in [5]. A PMS is used to obtain data for monitoring the system condition and selecting the active and reactive power settings for a local or dispersed power conditioning system (PCS) for the BESS. The ultimate goal of a PMS is maintaining the interoperability of the BESS with the operation strategies for an external electrical system implemented for reliability. The facilities for the demonstration research with a 4 MW and 8 MWh BESS at 'Jochun' was tested in the long-term and short-term cycle operation modes.

This paper proposes a real-time peak shaving algorithm that considers wind power generation. As in [6], the algorithm using a particular level of wind penetration employs the effective load curves, which are obtained by subtracting the wind generation from the load time series at each long-term cycle time unit. However, it should be noted that there are errors in the forecast load and wind generation values, and the real-time peak shaving operation might require a wind generation method with comparatively large forecasting errors. To effectively cope with the wind generation forecasting errors, this paper employs fuzzy wind power generation curves in a real-time algorithm for threshold value peak shaving. This paper includes illustrative examples to show the effectiveness of this real-time algorithm for peak shaving.

2. Peak Shaving Algorithm

The applicable schemes for using large-scale batteries in power systems can essentially be divided into long-term and short-term cycle modes. Peak shaving for an energy time shift can be considered to be the main function of battery energy storage in a long-term cycle operation. As in [5], several other long-term cycle operation functions could be described, considering system security. However, based on the purpose, the total state of charge (SOC) of the participating BESS modules with a PCS must be in an adequate range to be ready just in case, and the active and reactive power ordered by the PCS of the BESS can be used for system margin enhancement, loss minimization, etc. Short-term cycle operation with a BESS includes the mitigation of the fluctuating characteristic of renewable energy and frequency regulation with automatic generation control (AGC) or governor free (GF) actions.

In the literature, there are several approaches to peak shaving with energy storage devices. In [7], off-line and on-line peak shaving algorithms were described for a local load with renewable energy sources. The off-line algorithm can provide scheduling with the assumption that the real load curve is known in advance; the on-line algorithm might then include the uncertainty of the load curve. In [8], fundamental algorithms for peak shaving were proposed. In [9], a fuzzy load model for uncertain load curves was adopted in the scheduling formulation for peak shaving. In [9], a model predictive control method was employed to reduce the peak electricity demand in building climate control based on spot price forecasting. This paper describes a peak shaving method that determines a charging/discharging schedule to minimize the peak shaving threshold value, P_{shave}, considering the load data.

2.1 Charging/Discharging Model for BESS

To determine the charging and discharging schedule for the long-term cycle operation of the BESS, a BESS model is needed that explains the behavior for the given charging and discharging actions by the PCS in the system. The most important aspect of this model is the SOC characteristic, which depends on the active power injection and consumption.

Through the observation of the equivalent circuit from the viewpoint of the change in SOC during operation, the following difference equation can be obtained:

$$E_B(k+1) = (1-\gamma)E_B(k) - (1\pm\alpha)(1\pm\beta)P_B(k)\Delta T \quad (1)$$

where the following notations can be made:

$E_B(k)$: state of charge at k,

$P_B(k)$: power output at the point of k,

ΔT: long-term time unit (30 min),

α: coefficient of loss by converter loss,

β: coefficient of loss by battery current loss,

γ: coefficient of self-discharging.

In the model of Eq. (1), the loss terms totally depend on the active power output, which is the control input at each time period. As seen, two "±" signs are used for the loss coefficients in Eq. (1). If P_B(k) is positive, "+" is used; otherwise "-" is taken. It should be noted that a positive P_B(k) represents the discharging state. The difference Eq. (1) is adequate for the scheduling problem of peak and SMP shaving, because it explains the long-term cycle charging and discharging behaviors in terms of the change in the SOC of the BESS.

2.2 Peak Shaving Formulation

This subsection describes the fundamental peak shaving formulation. This algorithm is used to determine the charging and discharging schedule using the load data.

$$\begin{aligned} & \min P_{shave} - P_{fill} \\ & s.t.\ P_B(k) = P_L(k) - P_{shave} + P_{fill} \\ & \quad E_B(k+1) = (1-\gamma)E_B(k) \\ & \qquad\qquad - (1\pm\alpha)(1\pm\beta)P_B(k)\Delta T \\ & \quad P_{B_{\min}} \le P_B(k) \le P_{B_{\max}} \\ & \quad E_{B_{\min}} \le E_B(k) \le E_{B_{\max}} \\ & \quad E_B(M-1) = E_{B_o} \\ & \quad k = M, \cdots, N \end{aligned} \tag{2}$$

where P_{shave} is the threshold value for peak shaving, and P_{fill} is that for load filling. This algorithm has the purpose of minimizing P_{shave} during discharging periods and maximizing P_{fill} during charging periods. In Eq. (2) $P_L(k)$ denotes the load level at time k. In Eq. (2), M and N stand for the starting and ending times for the scheduling; $P_L(k)$ represent the scaled-down load level at time period k; $P_{B_{\min}}$ and $P_{B_{\max}}$ are the minimum and maximum designed power outputs, respectively; $E_{B_{\min}}$ and $E_{B_{\max}}$ are the minimum and maximum limits of the SOC, respectively, and corresponding constraints are needed to prevent over-charging and discharging; and E_{B_o} is the initial SOC right before the starting period of the scheduled discharge.

3. Wind Power Generation Forecasting Based on Fuzzy Modeling

In probability theory, a normal or Gaussian distribution is a very commonly occurring continuous probability distribution. Normal distributions are extremely important in statistics and are often used in the natural and social sciences for real-valued random variables whose distributions are unknown.

Different probability distribution functions may be selected for different kinds of uncertain values [10]. The normal distribution function is used in this paper. The general formula of the probability density function for a normal distribution with uncertain variable x is given below:

$$\begin{aligned} & f(x,\mu,\sigma) = \frac{1}{\sigma\sqrt{2\pi}} e^{-\frac{(x-\mu)^2}{2\sigma^2}} \\ & -\infty \le x \le \infty \\ & \sigma > 0 \end{aligned} \tag{3}$$

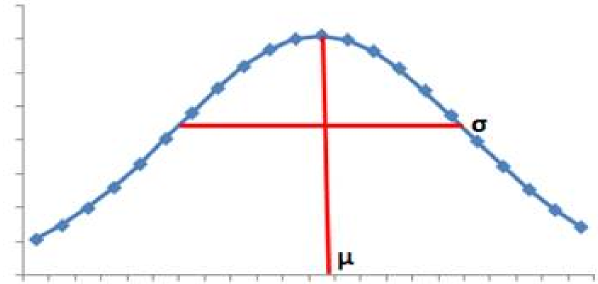

Figure 1. Normal distribution curve.

where x is the uncertain variable for the probability function; μ is the mean value of the uncertain value, also called the location parameter; and σ is the standard deviation of the uncertain value, also called the scale parameter. The shape of the plot of the normal probability density function is shown in Figure 1. In this paper, the normal distribution is converted into trapezoidal fuzzy curves with four discrete points. The normal distribution curve is constructed based on wind power generation data with a sampling time of 30 min.

Power load data, especially for residential loads, are variable and uncertain. For example, the variability of the electricity consumption of a single residential customer generally depends on whether family members are home and on the time of use of a few high-power appliances with relatively short usage durations during the day, and is subject to very high uncertainty. Probabilistic analysis and fuzzy theory can be used to analyze the uncertainty of the load [11].

A method for describing a membership function involves the application of data on the average value m and maximum error e of the input quantity. In practical applications, this method may be used to describe the values of wind power generation. In this case, the fuzzy parameters can be defined as follows [12]:

$$\begin{aligned} & fuzzy(1) = \mu - e \\ & fuzzy(2) = \mu - \frac{e}{2} \\ & fuzzy(3) = \mu + \frac{e}{2} \\ & fuzzy(4) = \mu + e \end{aligned} \tag{4}$$

where e is the maximum error.

A trapezoidal fuzzy curve can be drawn using Eq. (4) and is shown in Figure 2. This paper calculates the fuzzy percentage using this curve. Four fuzzy forecasting wind power generation curves are made using these percentages. The formula for

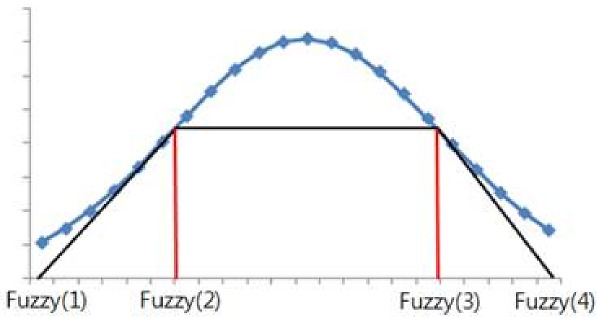

Figure 2. Trapezoidal fuzzy model derived from given normal distribution function.

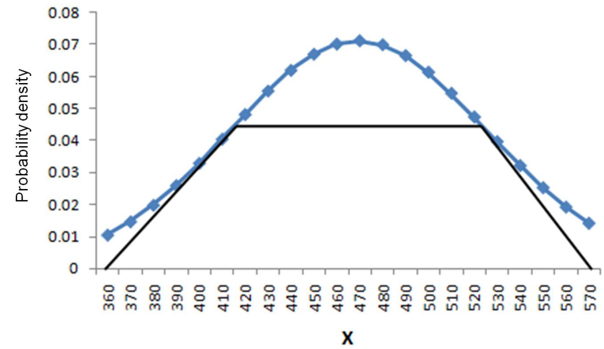

Figure 3. Normal distribution and trapezoidal fuzzy curves for wind power generation.

calculating the percentage is as follows:

$$Percentage(j) = \frac{fuzzy(j) - \mu}{\mu} \times 100[\%] \tag{5}$$
$$fuzzy(j): \text{ Fuzzy value in Eq. (4)}, j = 1, \cdots, 4$$

Wind power generation data are forecast using these four fuzzy forecasting wind power generation curves for real-time peak shaving. If the real wind power generation at an arbitrary point is smaller than the value of $fuzzy(1)$, the real-time peak shaving algorithm chooses the $fuzzy(1)$ wind power generation curve after this arbitrary point. Similarly, if the real wind power generation at an arbitrary point is greater than the value of $fuzzy(4)$, the real-time peak shaving algorithm chooses the $fuzzy(4)$ wind power generation curve after this arbitrary point. However, if the real wind power generation is in the region of $fuzzy(1)$-(4), the method used to forecast the wind power generation changes. For example, if the real wind power generation is located in the region of $fuzzy(1)$-(4), the algorithm calculates the percentage of real values from the nearest point, which becomes the starting point of the forecast wind power generation.

In the real-time operation, the applied level of wind generation is based on the fuzzy wind model at the following time period, which depends on the wind generation level at the previous long-term time unit. When the error between the real and forecast wind generation values is less than $fuzzy(1)$ at the previous time unit, the wind generation is set to the lowest wind generation corresponding to the value with the error of $fuzzy(1)$. When the error is between $fuzzy(1)$ and $fuzzy(2)$ or between $fuzzy(3)$ and $fuzzy(4)$, the wind generation level with the same fuzzy membership value is chosen. When the error is between $fuzzy(2)$ and $fuzzy(3)$, the wind generation level with the same distance from $fuzzy(2)$ is employed. When the error is greater than $fuzzy(4)$, the wind generation is set to the largest level in the fuzzy wind model. This forecasting is performed for the following long-term time periods.

4. Simulation and Results

This section describes the process of creating the trapezoidal fuzzy curve and gives corresponding examples of the application of the peak shaving algorithm. The wind power generation was classified on an hourly basis to generate the trapezoidal fuzzy curve and each fuzzy percentage. Thereafter, a normal distribution was made using the wind power generation data with respect to time. Figure 3 shows a trapezoidal fuzzy curve that was drawn using this method. The fuzzy model might have different values over the entire period. This paper uses a 48×4 matrix that includes the end-points of the trapezoidal models at all the periods using historical power generation data with 30-min intervals. Table 1 lists the percentages of the end-points of the fuzzy model at each time period in reference to the expectation, as determined in this paper.

The same fuzzy model could also be applied to load curves, as in [7]. However, in [7], the method used for the fuzzy model construction was not mentioned. This paper adds wind power generation data to the grid and performs real-time peak shaving under the assumption that the real load data are obtained. This paper illustrates the applicability of a fuzzy curve for wind power generation data. Figures 4 and 5 show the real load curve and real wind power generation curve, respectively. Figure 6 shows four fuzzy curves based on the forecast wind power generation curve. In Figures 4–6, the x-axis denotes the long-term time unit (30 min) intervals over the course of a day.

Table 1. Percentages of end-points of fuzzy model for wind power generation

Time unit	Fuzzy 4 (%)	Fuzzy 3 (%)	Fuzzy 2 (%)	Fuzzy 1 (%)
1	32.596	16.298	-16.298	-32.596
2	31.063	15.531	-15.531	-31.063
3	29.529	14.764	-14.764	-29.529
4	30.207	15.103	-15.103	-30.207
5	30.885	15.442	-15.442	-30.885
6	30.916	15.458	-15.458	-30.916
7	30.946	15.473	-15.473	-30.946
8	30.183	15.091	-15.091	-30.183
9	29.421	14.71	-14.71	-29.421
10	28.088	14.044	-14.044	-28.088
11	26.756	13.378	-13.378	-26.756
12	27.747	13.873	-13.873	-27.747
13	28.739	14.369	-14.369	-28.739
14	30.22	15.11	-15.11	-30.22
15	31.701	15.85	-15.85	-31.701
16	32.201	16.1	-16.1	-32.201
17	32.701	16.35	-16.35	-32.701
18	31.648	15.824	-15.824	-31.648
19	30.596	15.298	-15.298	-30.596
20	31.402	15.701	-15.701	-31.402
21	32.209	16.104	-16.104	-32.209
22	27.639	13.819	-13.819	-27.639
23	23.07	11.535	-11.535	-23.07
24	21.678	10.839	-10.839	-21.678
25	20.287	10.143	-10.143	-20.287
26	20.734	10.367	-10.367	-20.734
27	21.18	10.59	-10.59	-21.18
28	21.523	10.761	-10.761	-21.523
29	21.866	10.933	-10.933	-21.866
30	23.334	11.667	-11.667	-23.334
31	24.801	12.4	-12.4	-24.801
32	30.303	15.151	-15.151	-30.303
33	35.805	17.902	-17.902	-35.805
34	41.757	20.878	-20.878	-41.757
35	47.71	23.855	-23.855	-47.71
36	44.635	22.317	-22.317	-44.635
37	41.559	20.779	-20.779	-41.559
38	41.383	20.691	-20.691	-41.383
39	41.208	20.604	-20.604	-41.208
40	37.661	18.83	-18.83	-37.661
41	34.114	17.057	-17.057	-34.114
42	35.815	17.907	-17.907	-35.815
43	37.515	18.757	-18.757	-37.515
44	38.47	19.235	-19.235	-38.47
45	39.425	19.712	-19.712	-39.425
46	36.841	18.42	-18.42	-36.841
47	34.258	17.129	-17.129	-34.258
48	33.427	16.713	-16.713	-33.427

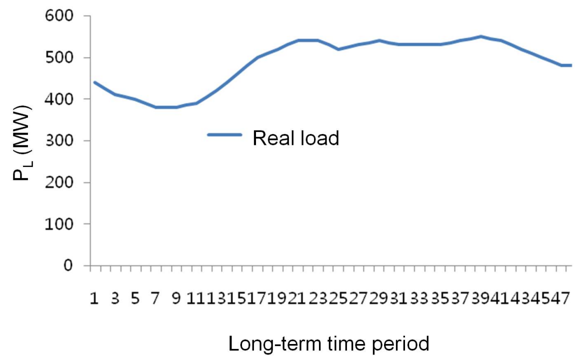

Figure 4. Example of real load curve.

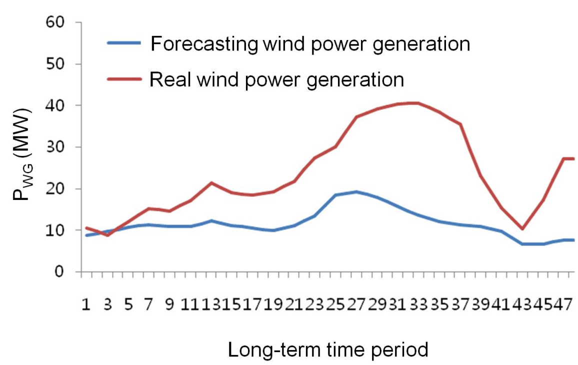

Figure 5. Example of wind power generation curves.

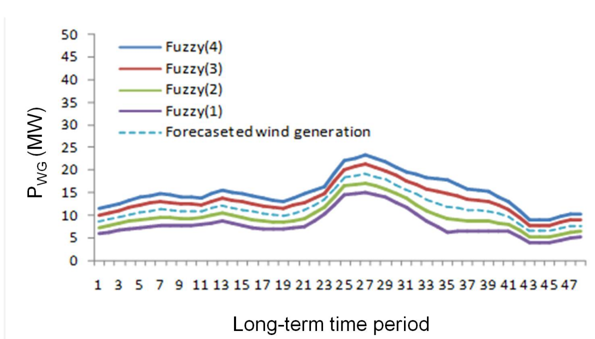

Figure 6. Trapezoidal fuzzy model based on expected wind power generation curve.

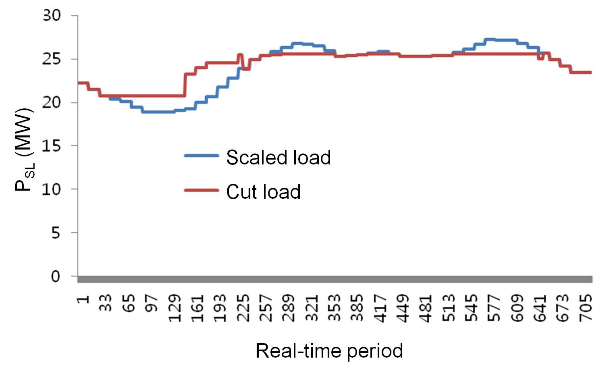

Figure 7. Peak shaving results using real wind power generation curve.

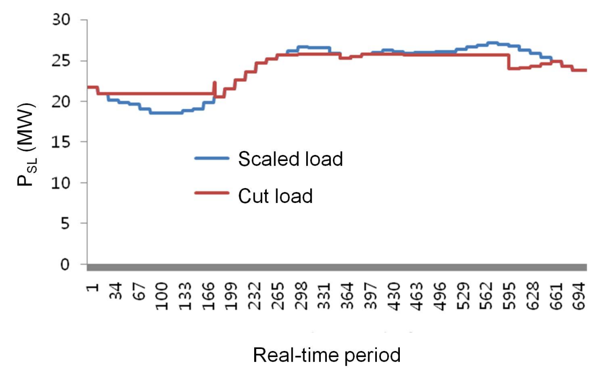

Figure 8. Peak shaving results using forecast wind power generation curve.

Figure 7 shows the peak shaving results using real load and real wind power generation data. Figure 8 illustrates the peak shaving results using real load and forecast wind power generation data. Figure 9 shows the peak shaving results using real load and wind power generation data after the application of the fuzzy model. In Figures 7–9, the x-axis denotes the real-time unit (2 min). This paper reports a real-time peak shaving simulation that divides the long-term time unit into 10 sections because the fuzzy wind power generation changes as a result of the real wind power generation data at each point. In other words, Figures 7–9 show the combined peak shaving results at the corresponding real-time units.

In a real-time simulation performed using the developed real-time mode emulator, one day is divided into five portions, and each portion starts from an long-term time unit: 1, 11, 21, 31, or 41. This is because different errors are expected between the real and forecast values of the wind power generation data at each portion. In other words, the error rate might be different depending on the time of day. Table 2 lists the error at each long-term section, 1–10, 11–20, 21–30, 31–40, and 41–48, compared to the results when using the real wind power generation data. In the process of peak shaving, the effective load was adopted, which is the load subtracted by the wind power generation. As listed in the table, the error rates at each section are smaller

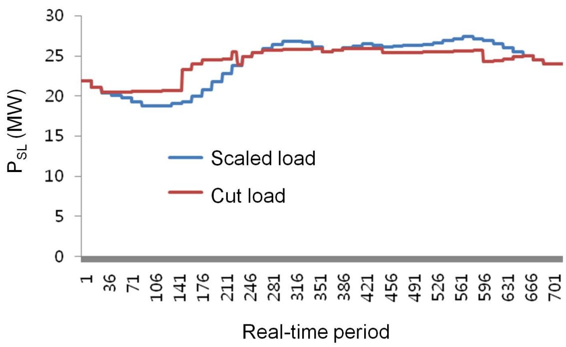

Figure 9. Peak shaving results using fuzzy model of wind power generation.

Table 2. Error rate of peak shaving results

LT time unit	Error rate (%)			
	Using real and forecast data		Using real and fuzzy data	
	Scaled load	Cut load	Scaled load	Cut load
1–10	1.92	1.10	1.14	1.12
11–20	0.67	6.38	0.19	0.39
21–30	0.76	0.84	1.31	1.17
31–40	2.02	0.93	2.72	0.23
41–48	1.28	2.97	1.21	2.67
Average	1.33	2.44	1.31	1.11

LT, long-term.

when using the fuzzy model of wind power generation. The same characteristic is seen in the overall error rate.

5. Conclusions

This paper presented long-term cycle control strategies for a large-scale BESS. The main focus of this paper was illustrating the applicability of a fuzzy model for the forecast wind power generation as an input for real-time peak shaving. This operation mode could be used to perform an energy time shift, and minimize the threshold value obtained from the difference between the upper and lower loads. This paper included an illustrative example showing the performance of the algorithm with real load and wind power generation data using real, forecast, and fuzzy model-based curves with the developed real-time operation simulator.

Conflict of Interest

No potential conflict of interest relevant to this article was reported.

References

[1] Electric Power Research Institute, "Electricity energy storage technology options," Available http://www.epri.com/abstracts/pages/productabstract.aspx?ProductID=000000000001020676

[2] J. Eyer and G. Corey, *Energy Storage for the Electricity Grid: Benefits and Market Potential Assessment Guide: A Study for the DOE Energy Storage Systems Program [SAND2010-0815]*, Albuquerque, NM: Sandia National Laboratories, 2010.

[3] J. B. Goodenough, H. D. Abruna, and M. V. Buchanan, *Basic Research Needs for Electrical Energy Storage. Report of the Basic Energy Sciences Workshop on Electrical Energy Storage [DOE/SC/BES-0702]*: U.S. Department of Energy, 2007.

[4] R. Lasseter and M. Erickson, *Integration of Battery-Based Energy Storage Element in the CERTS Microgrid [DE-FC02-06CH11350]*: US Department of Energy, 2009.

[5] H. Song, S. Ohn, S. Lee, and B. Jang, "Long-term cycle scheduling algorithms in power management system for MW-scale batteries," in *Proceedings of the IEEE Vehicle Power and Propulsion Conference*, Seoul, Korea, October 9-12, 2012, pp. 1006-1009. http://dx.doi.org/10.1109/VPPC.2012.6422754

[6] A. Bar-Noy, M. Johnson, and O. Liu, "Peak shaving through resource buffering," in *Approximation and Online Algorithms. Lecture Notes in Computer Science, Vol. 5426*, E. Bampis and M. Skutella, Eds. Heidelberg: Springer Berlin, 2009, pp. 147-159. http://dx.doi.org/10.1007/978-3-540-93980-1_12

[7] S. Ohn, J. S. Kim, H. Song, and B. Chang, "Fuzzy LP based power network peak shaving algorithm," *Journal of Korean Institute of Intelligent Systems*, vol. 22, no. 6, pp. 754-760, Dec. 2012. http://dx.doi.org/10.5391/JKIIS.2012.22.6.754

[8] S. B. Son, H. Song, and B. Chang, "Long-term cycle scheduling algorithms of peak-shaving for MW-scale battery energy storage system," in *Proceedings of the International Smart Grid Conference & Exhibition*, 2013, vol. 1, pp. 727-732.

[9] F. Oldewurtel, A. Ulbig, A. Parisio, G. Andersson, and M. Morari, "Reducing peak electricity demand in building climate control using real-time pricing and model predictive control," in *Proceedings of the 49th IEEE Conference on Decision and Control*, Atlanta, GA, December 15-17, 2010, pp. 1927-1932. http://dx.doi.org/10.1109/CDC.2010.5717458

[10] S. M. Ross, *Introduction to Probability Models*, 10th ed., Boston, MA: Academic Press, 2010.

[11] J. Zhu, *Optimization of Power System Operation*, Piscataway, NJ: Wiley-IEEE, 2009.

[12] J. Nazarko and W. Zalewski, "The fuzzy regression approach to peak load estimation in power distribution systems," *IEEE Transactions on Power Systems*, vol. 14, no. 3, pp. 809-814, Aug. 1999. http://dx.doi.org/10.1109/59.780890

Subin Son received B.S. in Electrical and Information Engineering from Seoul National University of Science & Technology in 2013. He is a graduate student at Seoul National University of Science & Technology. His research areas of interest are T&D application of battery energy storage systems, and power system operation.
Phone: +82-2-970-9873
E-mail: subregas@seoultech.ac.kr

Hwachang Song received B.S., M.S. and Ph.D. in Electrical Engineering from Korea University in 1997, 1999 and 2003, respectively. He was a post-doctoral visiting scholar at Iowa State University from 2003 to 2004. He was working as a faculty member in the School of Electronic and Information Engineering, Kunsan National University, from 2005 to 2008. Currently, he is an associate professor in the Department of Electrical and Information Engineering, Seoul National University of Science & Technology. His research areas of interest are nonlinear optimization, power system stability and control, battery energy storage systems, and system modeling.
Phone: +82-2-970-6402
E-mail: hcsong@seoultech.ac.kr